DYNAMIC BEHAVIOUR OF RAILWAY BRIDGES UNDER MOVING MASS LOAD – ITERATIVE MODAL ANALYSIS

Milan MORAVČÍK[1]

[1] Faculty of Civil Engineering, University of Žilina, Univerzitná 8215/1, 010 26 Žilina

milan.moravcik@fstav.uniza.sk

DOI: 10.35181/tces-2019-0018

Abstract. *Travelling mass due to its mass inertia has significant effect on the dynamic response of the bridges. This study is devoted to the study of the dynamic response the real steel railway bridge of the length L_b = 38 m for the single locomotive bogie mass load M_{Lbg} = 44 t (Škoda 350) passing over the bridge with the speed v=65 m/s. The iteration method of the governing partial differential equation of the transverse motion of the bridge structure w(x,t) has been applied. The modal superposition method for the vertical bridge deflection w(x,t) considering the first mode j=1 was used.*

Keywords

Dynamics of bridges, modal analysis, mass load.

1. Introduction

Investigating of railway bridges traversed by moving vehicles is one of the important concerns for the structural engineers in the design of highway and railway bridges. By introducing the inertial effects of the moving loads into the problem formulation, more realistic results would be gained especially for loads with relative large weights travelling at high speed.

When creating a computational model for a moving load–bridge, there is important the ratio of the bridge weight m_b and the weight of moving vehicle M_v and the speed c of the moving load. With regard to this aspect we say about the load models:

- moving load models, Fig. 1a,
- moving mass un-sprung and sprung models, Fig. 1b,
- a complex dynamic interaction model for the vehicle, Fig. 1c.

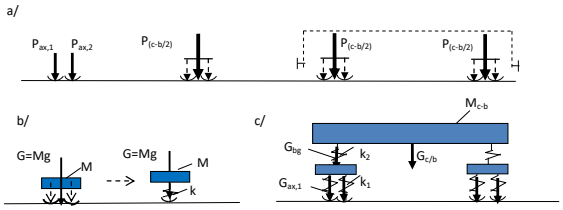

Fig. 1: Schematic representation of load models for the dynamic response of bridges.

For the load by a real train composed of several cars, or a characteristic vehicle there are applied different geometrical intervals for the set of loads, as is shown in Fig. 2.

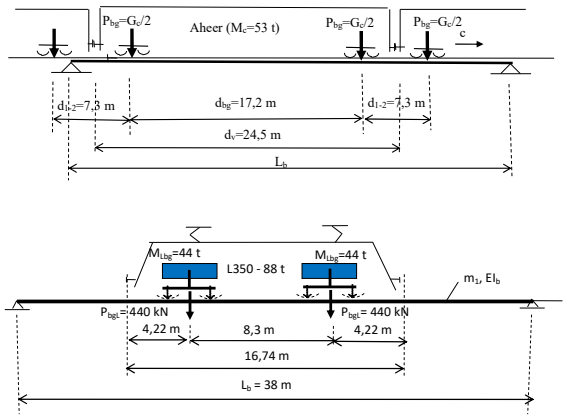

Fig. 2: Characteristic load of railway bridges – loading by IC cars and towing locomotive.

The basic role of the dynamic response of a bridge results from the analysis of a characteristic load concentrated at the bogie position of the locomotive. As a plain model is considered in the analysis the rolling of vehicles are neglected.

This study is devoted to the study of the dynamic response the real railway middle span bridge of the length L_b = 38 m for the single load M_{Lbg} = 44 kN moving the speed c = 65 m/s =234 km/h, Fig, 3. For the presented example the ratio of the moving mass and the beam mass m_b is M_{Lbg} / m_b = 0,36.

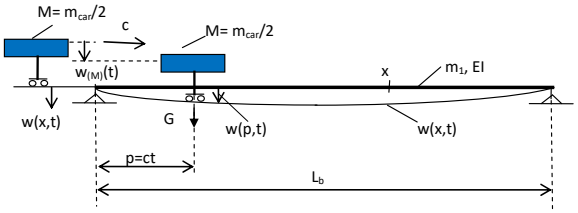

Fig. 3: Single mass M moving on the bridge.

2. Dynamic Equilibrium Equation and Solution

The main difficulty to deal with moving mass problems is that the unknown displacement $w(x,t)$ in the differential equation appears on the both sides of Eq. (1).

$$m_1 \frac{d^2w(x,t)}{dt^2} + EI\frac{d^4w(x,t)}{dx^4} = M(g - \ddot{w}_{(M)}(x,t)) \cdot \delta(x-ct) \quad (1)$$

where:

m_1 [t] is the mass per unit length of the bridge,

EI [kNm^2] is the bending stiffness of the bridge,

$\delta(x-ct)$ is the Dirac function (a generalized function expresses the concentrated load acting at point $p = x - ct$,

$\ddot{w}_{(M)}(x,t)$ is the vertical acceleration of the beam.

The force effect on the right hand side of Eq. (1) is acting in a moving coordinate $p = ct$, that is the instantaneous spatial location of the moving mass, can be expressed as

$$\frac{d^2w_{(M)}(p,t)}{dt^2} = \left(\frac{\partial^2 w(x,t)}{\partial t^2} + 2c\frac{\partial w(x,t)\cdot\partial w(x,t)}{\partial t \partial x} + c^2\frac{\partial^2 w(x,t)}{\partial x^2}\right) \quad (2)$$

The second and third term in Eq. (2) which are related to the Coriolis force and the centrifugal force are usually omitted on the dynamic response without affecting the accuracy of solution. Then the vertical component $\frac{\partial^2 w(x,t)}{\partial t^2}$ is considered and the problem is represented by the simplified equation

$$m_1\frac{d^2w(x,t)}{dt^2} + EI\frac{d^4w(x,t)}{dx^4} = \left(G - M(\frac{\partial^2 w(x,t)}{\partial t^2})\right)\delta(x-ct). \quad (3)$$

A convenient rigorous solution for the problem has not been found. Commercial finite element solvers applied to the moving mass are also questionable. Therefore an iterative approach was applied. Equation (3) for an iteration approach can be rewriting as

$$m_1\frac{d^2w^{(k)apx}(x,t)}{dt^2} + EI\frac{d^4w^{(k)apx}(x,t)}{dx^4} = F^{(k)\text{apx}}(t)\cdot\delta(x-ct). \quad (4)$$

The interaction force (the contact force) is

$$F^{(\text{k})\text{apx}}(t) \equiv M(g - \ddot{w}^{(k-1)apx}_{(M)}(p,t))\cdot\delta(p-ct) \quad (5)$$

The interaction force (the contact force) in Eq. (5) is the superposition of the gravity force G=mg and the inertia force $M\cdot\ddot{w}^{(k-1)\text{apx}}_{M}(p,t)$ due to acceleration of the mass M.

The modal superposition method for the vertical bridge deflection $w(x,t)$ considering the first mode j=1 was applied:

$$w_{(1)}(x,t) = q_{(1)}(t)\phi_{(1)}(x) \quad (6)$$

Then, the interaction force Eq. (5) can be expressed by mean the modal coordinate $q_{(1)}(t)$ as

$$F^{(k)apx}_{(1),(G+M)}(t) = G^{(k)apx} - M\cdot\ddot{w}^{(k-1)apx}_{(1)}(p,t) = G - M\cdot\ddot{q}^{(k-1)\text{apx}}_{(1)}(t)\cdot\sin\Omega_{(1dr}t \quad (7)$$

The modal equation corresponding Eq. (1) and Eq. (7) after manipulations [3] can be written as [2,3,5]

$$\ddot{q}^{(k)apx}_{(1)}(t) + \omega^2_{(1)}q^{(k)apx}_{(1)}(t) = \frac{F^{(k)apx}_{(1),(G+M)}(t)\cdot\phi_{(1)}(x)}{m_1\int_0^{L_b}\phi^2_{(1)}(x)dx} \quad (8)$$

The modal equation (8) in practical solution is applied for the fundamental mode of vibration j=1 and for the mass force (7) it may be written as

$$\ddot{q}^{(k)apx}_{(1)}(t) + \omega^2_{(1)}q^{(k)apx}_{(1)}(t) = \frac{2F^{(k)apx}_{(1),(G+M)}(t)\cdot\sin\Omega_{(1(dr}t}{m_1L_b} \quad (9)$$

or by means the modal coordinate Eq. (7) has the form

$$\ddot{q}_{(1)}(t) + \omega^2_{(1)}q_{(1)}(t) = \frac{2\cdot G}{m_1L_b}\sin\Omega_{(1)\text{dr}}t - \frac{2\cdot M}{m_1L_b}\ddot{q}_{(1)}(t)\cdot(\sin\Omega_{(1)\text{dr}}t)^2 \quad (10)$$

Eq. (10) is the nonlinear equation and the rigorous solution has not been found. Equation (10) is valid because it is assumed that the contact of mass M and the beam is always maintained, i.e. the acceleration of the beam $\ddot{w}_{(1)}(p,t)$ and the acceleration of the mass $\ddot{w}_{(\text{M})}(p,t)$ are the same:

$$\ddot{w}^{(k-1)apx}_{(M)}(p,t) = \ddot{w}^{(k-1)apx}_{(1)}(p=ct,t) \quad (11)$$

Then, the interaction force can be considered as the superposition of effects of the gravitation force and the inertia force:

$$F^{(k)\text{apr}}(t) = F^{(k)\text{apr}}_{(G)}(t) + F^{(k)\text{apr}}_{(M)}(t) = G + F^{(k)\text{apr}}_{(M)}(t). \quad (12)$$

The modal Eq. (10), for the known interaction force $F^{(k)\text{apr}}(t)$, can be solved in the time domain by the convolution integral and the modal coordinate $q^{(k)apx}_{(1)}(t)$ considering the I^{st} mode of vibration is

$$q^{(k)apx}_{(1)}(t) = \frac{1}{\omega_{(1)}}\int_0^t\left[\frac{2F^{(k)apx}(t)}{m_1L_b}\sin\Omega_{(1)dr}(\tau)\right]\sin\omega_{(1)}(t-\tau)d\tau \quad (13)$$

3. Iteration Solution of Interaction Forces and Displacements

- **Inputs parameters for the numerical example**: G_{bg} = 440 kN, c = 65 m/s = 234 km/h, L_b = 38 m.
- **Bridge structure**

  - the bending stiffness $EI = 7.58 \cdot 10^7$ kNm^2,

  - the beam mass $m_1 = m_{1(BS)} + m_{1(Sup)}$ = 3180 kg/m,

  - the first circular frequency $\omega_{(1)} = 33.34 s^{-1}$,

  - the driving frequency $\Omega_{(1)dr} = \dfrac{\pi c}{L_b} = 5.3711\,[\mathrm{s}^{-1}]$,

  - the dimensionless speed factor

$$\alpha_{(1)} = \frac{\Omega_{(1)dr}}{\omega_{(1)}} = 0.1611 \cdot$$

The numeric solution is processed with [6].

3.1 First Interaction (k=1)

This load state corresponds to the simple moving force $G_{L_{bg}}$ over the bridge, Fig. 4.

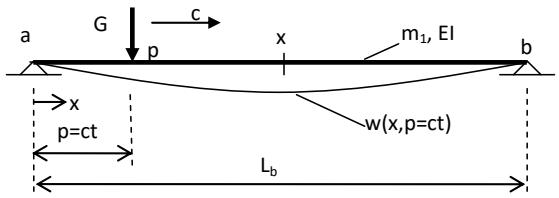

Fig. 4: Load model for the first iteration.

1) Interaction force due to the gravity force

The first interaction force acting on the beam at any distance $p = ct$, Fig. 4, is expressed from (3) without the inertial effect of the mass $M_{(L_{bg})}$ as

$$F^{1apx}_{(G_{bg})}(p,t) = G_{L_{bg}} = 440 kN\,. \qquad (14)$$

2) Modal displacement due to gravity force

The general modal equation for $q^{1apx}_{(1),(G_{L_{bg}})}(t)$ due to the single gravitation force $G_{L_{bg}}$, resulting from the differential equation Eq. (10), is the known modal equation due to moving force [2, 5]:

$$\ddot{q}^{1apx}_{(1),(G_{L_{bg}})}(t) + \omega^2_{(1)} q^{1apx}_{(1),(G_{L_{bg}})}(t) = \frac{2G_{L_{bg}}}{m_1 L_b} \sin \Omega_{(1)dr} t \qquad (15)$$

The analytical solution Eq. (15) [1, 4] is:

$$q^{1apx}_{(1),(G_{L_{bg}})}(t) = \frac{\hat{q}_{(1),(G_{L_{bg}})st}(L_b/2)}{1-\alpha^2_{(1)}} \left(\sin \Omega_{(1)dr} t - \alpha_{(1)} \sin \omega_{(1)} t\right) \qquad (16)$$

The modal displacement from Eq. (16) can be expressed by superposition of components:

$$q^{1apx}_{(1)(G_{L_{bg}})}(t) = q^{1apx}_{(1)(G_{L_{bg}})\mathrm{st}}(t) + q^{1apx}_{(1)(G_{L_{bg}})\mathrm{dyn}}(t) \qquad (17)$$

The mid-point beam displacement $w^{1apx}_{(1)(G_{L_{bg}})}(L_b/2,t)$ is identical with the modal displacement $q^{1apx}_{(1),(G_{L_{bg}})}(t)$:

$$w^{1apx}_{(1)(G_{L_{bg}})}(L_b/2,t) = q^{1apx}_{(1)(G_{L_{bg}})}(t) \cdot \sin \frac{\pi L_b}{2L_b} \equiv q^{1apx}_{(1)(G_{L_{bg}})}(t) \qquad (18)$$

Numerical results of the dynamic deflection at the midpoint of the bridge are presented in Fig. 5 ÷ Fig. 7.

3) Mid-point modal displacement $q^{1apx}_{(1),(G_{L_{bg}})}(t)$

- **Components of the modal displacement, Fig. 5.**

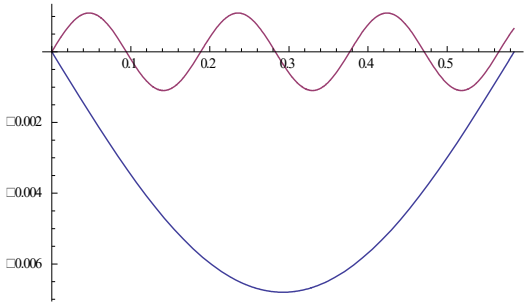

Fig. 5: Axes: x= t [s], y= Components $q^{1apx}_{(1),(G_{L_{bg}})\mathrm{st}}(t), q^{1apx}_{(1),(G_{L_{bg}})\mathrm{dyn}}(t)$

Amplitudes: $\hat{q}^{1apx}_{(1),(G_{L_{bg}})\mathrm{st}}(t) = 0{,}0068\,\mathrm{m}$, $\hat{q}^{1apx}_{(1),(G_{L_{bg}})\mathrm{dyn}}(t) = 0{,}0011\,\mathrm{m}$

The ratio of amplitudes: $\dfrac{\hat{q}^{1apx}_{(1),(G_{L_{bg}})\mathrm{dyn}}(t)}{\hat{q}^{1apx}_{(1),(G_{L_{bg}})st}(t)} = \dfrac{0.0011}{0.0067} = 0.16$ .....16 %

- **Total modal component $q^{1apx}_{(1),(G_{L_{bg}})}(t)$**, Fig. 6.

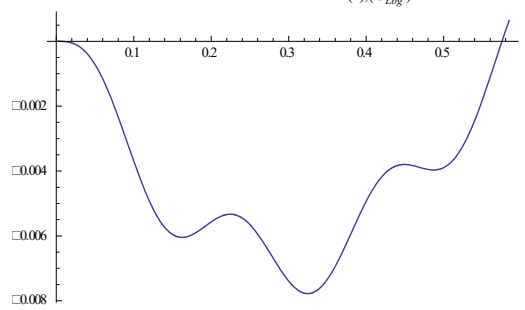

Fig. 6: Axes: x= t [s], y= $q^{1apx}_{(1),(G_{L_{bg}})}(t)$ [m], Amplitude:

$\hat{q}^{1apx}_{(1),(G_{L_{bg}})}(t) = 0.0076\,\mathrm{m}$

- **Dynamic coefficient δ^{1apr}_{dyn}**, Fig. 7.

In practice the dynamic coefficient is defined as the ratio of the maximum dynamic deflection to the static deflection at mid-span of a bridge. For (k=1) it is:

$$\delta^{1apr}_{dyn} = \frac{q^{1apx}_{(1),(G_{L_{bg}})}(t)_{\max}}{\hat{q}^{1apx}_{(1),(G_{L_{bg}})st}(t)} \qquad (19)$$

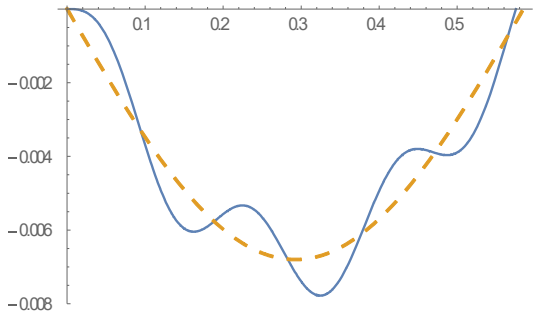

Fig. 7: Axes: x=t [s], y= Dynamic coefficient

$$\delta_{dyn}^{1apr} = \frac{q_{(1),(G_{Lbg})}^{1apx}(t)_{\max}}{\hat{q}_{(1),(G_{Lbg})st}^{1apx}(t)} = \frac{0.0076}{0.0067} = 1.13$$

4) **Beam displacement $w_{(1)(G_{Lbg})}^{1apx}(p,t)$ under the moving coordinate $p = ct$ and the modal displacement $w_{(1)(G_{Lbg})}^{1apx}(L_b/2,t)$**

The beam displacement $w_{(1)(G_{Lbg})}^{1apx}(p,t)$ under the moving force $F_{(G_{bg})}^{1apx}(p,t)$ is also defined by the modal coordinate $q_{(1),(G_{Lbg})}^{1apx}(t)$ and the result is in Fig. 8.

$$w_{(1)(G_{Lbg})}^{1apx}(p,t) = q_{(1),(G_{Lbg})}^{1apx}(t)\cdot\sin\Omega_{(1)dr}t \qquad (20)$$

The modal displacement $q_{(1),(G_{Lbg})}^{1apx}(t) \equiv w_{(1)(G_{Lbg})}^{1apx}(L_b/2,t)$ is known from Eq. (16), Fig. 6.

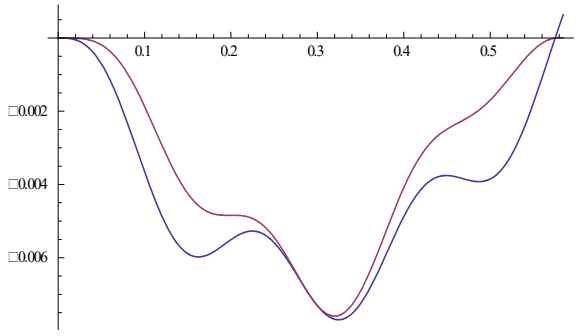

Fig. 8: Axes: x= t [s], y= $w_{(1)(G_{Lbg})}^{1apx}(p,t)$ [m] – the brick red color, $q_{(1),(G_{Lbg})}^{1apx}(t) \equiv w_{(1)(G_{Lbg})}^{1apx}(L_b/2,t)$ - the blue color,

3.2 Second Interaction (k=2)

This load state corresponds to the moving force $F_{(G_{Lbg}+M_{Lbg})}^{2apx}(p,t)$ due to load $(G_{L_{bg}}+M_{L_{bg}})$, (Fig. 3), can be solved by the superposition with the static contact force $F_{(G_{Lbg})}^{2apx}(p,t) = G_{L_{bg}}$ and the time-dependent dynamic force $F_{(M_{Lbg})}^{2apx}(p,t)$ is

$$F_{(G_{Lbg}+M_{Lbg})}^{2apx}(p,t) = G_{L_{bg}} + F_{(M_{Lbg})}^{2apx}(p,t). \qquad (21)$$

5) **Interaction force component due to the gravity force $G_{L_{bg}}$**

The gravitation force $F_{(G_{Lbg})}^{2apx}(p,t)$ for the bogie position $p = ct$ is given from input parameters as

$$F_{(G_{Lbg})}^{2apx}(p,t) = G_{(L_{bg})} = 440kN \qquad (22)$$

6) **Interaction force component due to the mass load $M_{(L_{bg})} = 44t$**

The interaction force due to mass $M_{L_{bg}} = 44t$ can be formulated direct from Eq. (10):

$$F_{(M_{Lbg})}^{2apx}(p,t) = -M_{(L_{bg})}\cdot\ddot{q}_{(1),(G_{Lbg}+M_{Lbg})}^{1apx}(t)\cdot\sin\Omega_{(1)dr}t =$$
$$= \hat{F}_{(M_{Lbg})}\left(-\Omega_{(1)dr}^2\cdot(\sin\Omega_{(1)dr}t)^2 + \Omega_{(1)dr}\omega_{(1)}\cdot\sin\omega_{(1)}t\cdot\sin\Omega_{(1)dr}t\right) \qquad (23)$$

The force component $F_{(M_{Lbg})}^{2apx}(p,t)$ contains two parts corresponding to the modal acceleration $\ddot{q}_{(1),(M_{Lbg})}^{1apx}(t) \equiv \ddot{q}_{(1),(G_{Lbg})}^{1apx}(t)$ from the first iteration of the mass $M_{(L_{bg})} = 44t$ and it can be express by the superposition:

$$F_{(M_{Lbg})}^{2apx}(p,t) = {}^{1}F_{(M_{Lbg})st}^{2apx}(p,t) + {}^{2}F_{(M_{Lbg})dyn}^{2apx}(p,t) \qquad (24)$$

Numerical results of the dynamic force and its components at the midpoint of the bridge are processed with [6] and presented are in Fig. 9 ÷ Fig. 11.

- **Quasi-static force component ${}^{1}F_{(M_{Lbg})st}^{2apx}(p,t)$ due acceleration ${}^{1}\ddot{q}_{(1),(G_{Lbg})st}^{1apx}(t)$**

This component results direct from Eq. (23), Fig. 9:

$${}^{1}F_{(M_{Lbg})st}^{2apx}(p,t) = M_{(L_{bg})}\frac{\hat{q}_{(1)(G_{Lbg})st}(L_b/2)}{1-\alpha_{(1)}^2}\Omega_{(1)dr}^2\cdot(\sin\Omega_{(1)dr}t)^2 \qquad (25)$$

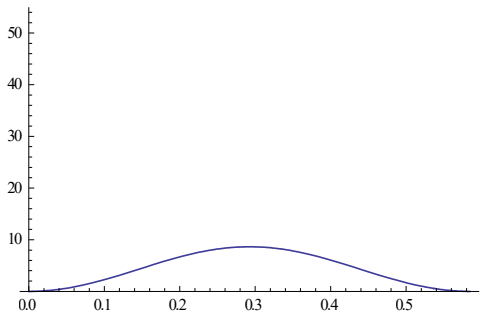

Fig. 9: Axes: x= t [s], y= ${}^{1}F_{(M_{Lbg})st}^{2apx}(t)$ [kN], ${}^{1}\hat{F}_{(M_{Lbg})st}^{2apx}(p,t) = 8,6kN$.

- **Dynamic force component ${}^{2}F_{(M_{Lbg})dyn}^{2apx}(p,t)$ due acceleration ${}^{2}\ddot{q}_{(1),(G_{Lbg})dyn}^{1apx}(t)$**

This component results direct from Eq. (23), Fig. 10:

$$ {}^{2}F^{2apx}_{(M_{Lbg})\mathrm{dyn}}(p=ct)=\left[-M_{(L_{bg})}\,{}^{2}\ddot{q}^{1apx}_{(1),(G_{Lbg})dyn}(t)\cdot\sin\Omega_{(1)dr}t\right]= \quad (26)$$

$$ =-M_{(L_{bg})}\frac{\hat{q}_{(1)(G_{Lbg})\mathrm{st}}(L_b/2)}{1-\alpha^2_{(1)}}\Omega_{(1)\mathrm{dr}}\omega_{(1)}\cdot\left(\sin\omega_{(1)}t\cdot\sin\Omega_{(1)dr}t\right)$$

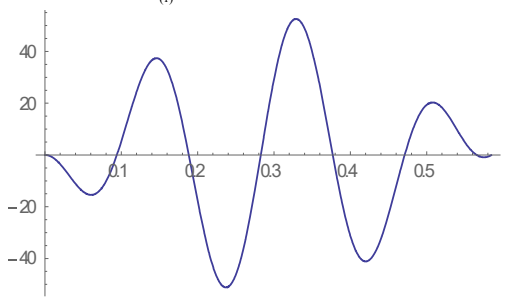

Fig. 10: Axes: x= t [s], y= ${}^{2}F^{2apx}_{(M_{Lbg})dyn}(p=ct)$ [kN], ${}^{2}\hat{F}^{2apx}_{(M_{Lbg})dyn}(p=ct)=52kN$.

- **Total inertial force effect $F^{2apx}_{(M_{Lbg})}(p,t)$ due to the mass $M_{L_{bg}}=44t$**

Superposition from Eq. 24 one obtains the total inertial effect $F^{2apx}_{(M_{Lbg})}(p,t)$ and its components:

- **Components ${}^{1}F^{2apx}_{(M_{Lbg})\mathrm{st}}(p,t)$ and ${}^{2}F^{2apx}_{(M_{Lbg})\mathrm{dyn}}(p,t)$ of the inertial force $F^{2apx}_{(M_{Lbg})}(p,t)$,** Fig. 11.

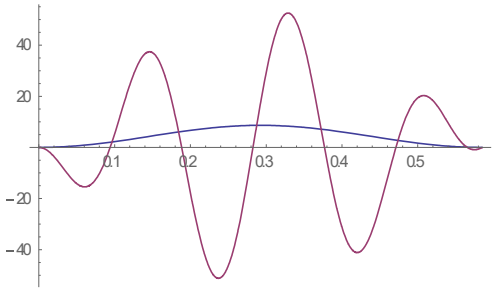

Fig. 11: Axes: x= t [s], y= ${}^{1}F^{2apx}_{(M_{Lbg})\mathrm{st}}(p,t)$, ${}^{2}F^{2apx}_{(M_{Lbg})dyn}(p,t)$ [kN],Amplitudes: ${}^{1}\hat{F}^{2apx}_{(M_{Lbg})\mathrm{st}}(p,t)=8.6kN$, ${}^{2}\hat{F}^{2apx}_{(M_{Lbg})dyn}(p,t)=52kN$.

From Fig. 11 can see the dominant effect generates the dynamic component ${}^{2}\hat{F}^{2apx}_{(M_{Lbg})dyn}(p,t)$.

- **Total inertial force $F^{2apx}_{(M_{Lbg})}(p,t)$,** Fig. 12.

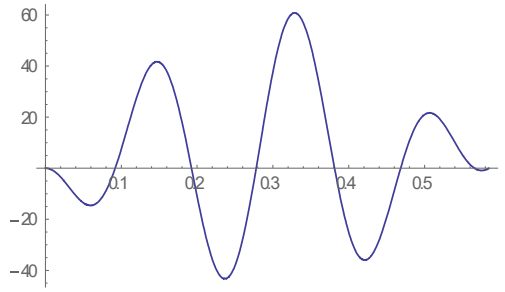

Fig. 12: Axes: x= t [s], y= Total force $F^{2apx}_{(M_{Lbg})}(t)$ [kN], Amplitudes $\hat{F}^{2apx}_{(M_{Lbg})}(p,t)$ = 60,5 kN.

7) Total modal displacement due to load $(G_{L_{bg}}+M_{L_{bg}})$

The influence of the interaction force of the locomotive bogie load $F^{2apx}_{(G_{Lbg}+\mathrm{M}_{Lbg})}(p,t)$ on the dynamic bridge deflection is evaluated though the modal displacement $q^{2apx}_{(1)(G_{Lbg}+\mathrm{M}_{Lbg})}(t)$:

$$ w^{2apx}_{(1)(G_{Lbg}+\mathrm{M}_{Lbg})}(p=ct,p)=q^{2apx}_{(1)(G_{Lbg}+\mathrm{M}_{Lbg})}(t)\cdot\sin\Omega_{(1)dt}t\,. \quad (27)$$

The total modal displacement $q^{2apx}_{(1)(G_{Lbg}+\mathrm{M}_{Lbg})}(t)$ can be expressed by the convolution integral:

$$ q^{2\mathrm{apx}}_{(1)}(t)=\frac{1}{\omega_{(1)}}\int_0^t\left[\frac{2F^{2apx}(p,t)}{m_1L_b}\sin\Omega_{(1)dr}\tau\right]\cdot\sin\omega_{(1)}(t-\tau)d\tau \quad (28)$$

This displacement is again advantageously to evaluate through modal components $q^{2apx}_{(1),(G_{Lbg})}(t)$ and $q^{2apx}_{(1),(\mathrm{M}_{Lbg})}(t)$ belong effects $G_{L_{bg}}$ and $M_{L_{bg}}$ by the superposition as

$$ q^{2apx}_{(1),(G_{Lbg}+\mathrm{M}_{Lbg})}(t)=q^{2apx}_{(1),(G_{Lbg})}(t)+q^{2apx}_{(1),(\mathrm{M}_{Lbg})}(t) \quad (29)$$

Results of solution of modal displacements due to the load $(G_{L_{bg}}+M_{L_{bg}})$ are shown in Figs. 13÷17.

- **Modal displacement $q^{2apx}_{(1),(G_{Lbg})}(t)$ due to the gravity force**

The modal displacement $q^{2apx}_{(1),(G_{Lbg})}(t)$ is expressed from Eq. (25) as

$$ q^{2apx}_{(1),(G_{Lbg})}(t)=\frac{1}{\omega_{(1)}}\int_0^t\left[\frac{2\cdot F^{2apx}_{(G_{bg})}(p)}{m_1L_b}\sin\Omega_{(1)dr}\tau\right]\cdot\sin\omega_{(1)}(t-\tau)d\tau=$$

$$ =\frac{1}{\omega_{(1)}}\frac{2}{m_1L_b}G_{(L_{bg})}\int_0^t\sin\Omega_{(1)dr}\tau\cdot\sin\omega_{(1)}(t-\tau)d\tau \quad (30)$$

For $\hat{q}^{2apx}_{(1),(G_{Lbg})}=\frac{1}{\omega_{(1)}}\frac{2}{m_1L_b}G_{(L_{bg})}=0.2148$ the modal displacement $q^{2apx}_{(1),(G_{Lbg}))}(t)$ is presented in Fig. 13.

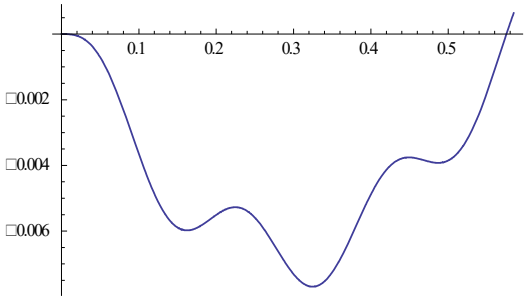

Fig. 13: Axes: x= t [s], y= $q^{2apx}_{(1),(G_{Lbg})}(t)$ [m], Amplitudes: $\hat{q}^{2apx}_{(1),(G_{Lbg})}(t)=0.0076m$

- **Modal displacement $q^{2apx}_{(1),(M_{Lbg})}(t)$ due to the inertial mass effect $M_{(L_{bg})} = 44t$**

This displacement can be also expressed by the convolution integral (the analogous practice as in the Section (3.2.3)), but now for the interaction inertial force $F^{2apx}_{(M_{Lbg})}(t)$ due to the acceleration $\ddot{w}^{2apx}_{(G_{Lbg})}(p,t)$:

$$q^{2apx}_{(1),(M_{Lbg})}(t)\frac{1}{\omega_{(1)}}\int_0^t\left[\frac{2\cdot F^{2apx}_{(M_{Lbg})}(t)}{m_1 L_b}\sin\Omega_{(1)dr}\tau\right]\cdot\sin\omega_{(1)}(t-\tau)d\tau \tag{31}$$

The loading force component $F^{2apx}_{(M_{Lbg})}(t)$ in Eq. (31) is the inertial force, which is the function of acceleration $\ddot{q}^{1apx}_{(1),(G_{Lbg})}(t)$ from the first iteration:

$$F^{2apx}_{(M_{Lbg})}(t) = -M_{(L_{bg})}\ddot{q}^{1apx}_{(1),(G_{Lbg})}(t) \tag{32}$$

The acceleration force component in Eq. (32) can be divided into parts:

$$\ddot{q}^{1apx}_{(1)(G_{Lbg})}(t) = {}^1\ddot{q}^{1apx}_{(1)(G_{Lbg})\mathrm{st}}(t) + {}^2\ddot{q}^{1apx}_{(1)(G_{Lbg})\mathrm{dyn}}(t) \tag{33}$$

Such superposition gives a quasi- static modal displacement ${}^1q^{2apx}_{(1),(M_{Lbg})\mathrm{st}}(t)$ and a dynamic modal displacement ${}^2q^{2apx}_{(1),(M_{Lbg})dyn}(t)$:

$$q^{1apx}_{(1)(G_{Lbg})}(t) = {}^1q^{1apx}_{(1)(G_{Lbg})\mathrm{st}}(t) + {}^2q^{1apx}_{(1)(G_{Lbg})\mathrm{dyn}}(t) \tag{34}$$

8) Quasi-static component ${}^1q^{2apx}_{(1),(M_{Lbg})\mathrm{st}}(t)$ of the modal displacement

The component ${}^1q^{2apx}_{(1),(M_{Lbg})\mathrm{st}}(t)$ of the modal displacement is expressed by the convolution integral and is presented in Fig. 14.
For

$${}^1\hat{q}^{*2apx}_{(1),(M_{Lbg})\mathrm{st}} = \frac{1}{\omega_{(1)}}\frac{2}{m_1 L_b}M_{(L_{bg})}\frac{\hat{q}_{(1)(G_{Lbg})\mathrm{st}}(L_b/2)}{1-\alpha^2_{(1)}}\Omega^2_{(1)dr} = 0,0043$$

$${}^1q^{2apx}_{(1),(M_{Lbg})\mathrm{st}}(t) = {}^1\hat{q}^{2apx}_{(1),(M_{Lbg})\mathrm{st}}\int_0^t \sin\Omega_{(1)dr}\tau)^2\cdot\sin\omega_{(1)}(t-\tau)d\tau \tag{35}$$

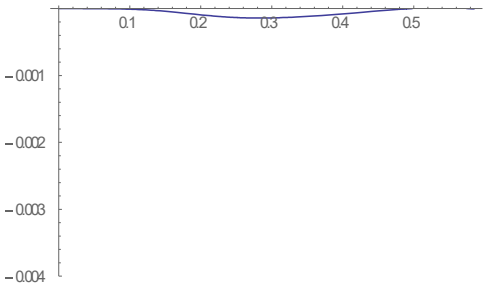

Fig. 14: Axes: x= t [s], y= ${}^1q^{2apx}_{(1),(M_{Lbg})\mathrm{st}}(t)$ [m], Amplitude: ${}^1\hat{q}^{2apx}_{(1),(M_{Lbg})\mathrm{st}}(t) = 0.00014m$.

9) Dynamic component of the modal displacement ${}^2q^{2apx}_{(1),(M_{Lbg})dyn}(t)$

For the amplitude of the modal displacement

$${}^2\hat{q}^{*2apx}_{(1),(M_{Lbg})dyn} = \frac{1}{\omega_{(1)}}\frac{2}{m_1 L_b}M_{(L_{bg})}\frac{\hat{q}_{(1)(G_{Lbg})\mathrm{st}}(L_b/2)}{1-\alpha^2_{(1)}}\Omega_{(1)dr}\omega_{(1)} = 0.0266 \tag{36}$$

The modal displacement component ${}^1q^{2apx}_{(1),(M_{Lbg})\mathrm{st}}(t)$ is again expressed by the convolution integral and the result is shown in Fig. 15.

$${}^2q^{2apx}_{(1),(M_{Lbg})\mathrm{dyn}}(t) = -{}^2\hat{q}^{2apx}_{(1),(M_{Lbg})\mathrm{dyn}}\int_0^t\left(\sin\omega_{(1)}\tau\cdot\sin\Omega_{(1)dr}\tau\right)\cdot\sin\omega_{(1)}(t-\tau)d\tau \tag{37}$$

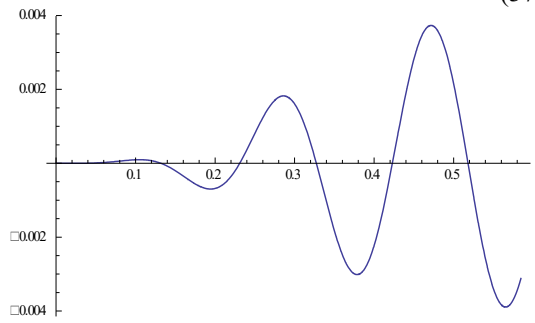

Fig. 15: Axes: x= t [s], y= ${}^2q^{2apx}_{(1),(M_{Lbg})dyn}(t)$ [m], Amplitude ${}^2\hat{q}^{2apx}_{(1),(M_{Lbg})dyn}(t) = 0,0039m$.

10) Total modal displacement $q^{2apx}_{(1),(M_{Lbg})}(t)$

Superposition from Eq. (34) one get the total modal displacement $q^{2apx}_{(1),(M_{Lbg})}(t)$ with its components.

- **Components $q^{2apx}_{(1),(M_{Lbg})\mathrm{st}}(t), q^{2apx}_{(1),(M_{Lbg})\mathrm{dyn}}(t)$**, Fig. 16.

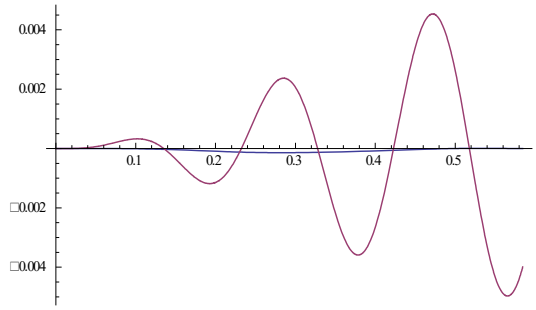

Fig. 16: Axes: x= t [s], y= Components ${}^1q^{2apx}_{(1),(M_{Lbg})\mathrm{st}}(t)$, ${}^2q^{2apx}_{(1),(M_{Lbg})\mathrm{dyn}}(t)$ of the modal displacement $q^{2apx}_{(1),(M_{Lbg})}(t)$ [m].

- **Total inertial mass effect $q^{2apx}_{(1)(M_{Lbg})}(t)$**, Fig. 17.

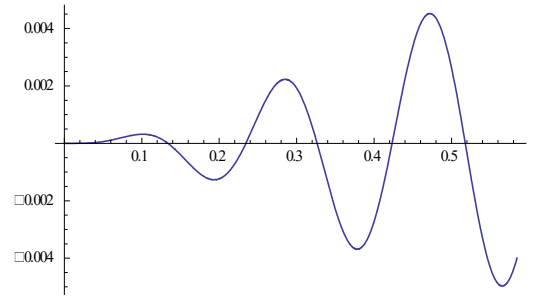

Fig. 17: Axes: x= t [s], y= Total displacement $q^{2apx}_{(1),(M_{Lbg})}(t)$ [m], Amplitude ${}^2\hat{q}^{2apx}_{(1),(M_{Lbg})dyn}(t) = 0.0039m$.

From Fig. 16 can be seen that for the dominant effect of the dynamic component ${}^{2}w^{2apx}_{(M_{Lbg})dyn}(p,t)$ can be stated:

$$w^{2apx}_{(M_{Lbg})}(p,t) \approx {}^{2}w^{2apx}_{(M_{Lbg})dyn}(p,t) \tag{38}$$

11) Beam displacement at midpoint due to load $(G_{L_{bg}} + M_{L_{bg}})$ and for the speed c = 65 m/s

The beam displacement $w^{2apx}_{(1)(G_{Lbg}+M_{Lbg})}(L_b/2,t)$ at the midpoint due to the force $F^{2apx}_{(G_{bg}+M_{Lbg})}(p,t)$ is also defined by the modal coordinate $q^{1apx}_{(1),(G_{Lbg})}(t)$.

$$w^{2apx}_{(1)(G_{Lbg}+M_{Lbg})}(L_b/2,t) = q^{2apx}_{(1)(G_{Lbg})}(t)\cdot\sin\Omega_{(1)dr}t \tag{39}$$

The beam displacement at mid-point of the beam $w^{2apx}_{(1),(G_{(Lbg)}+M_{Lbg})}(L_b/2,t)$ obtains also by the superposition.

$$w^{2apx}_{(1)(G_{Lbg}+M_{Lbg})}(L_b/2,t) = w^{2apx}_{(1),(G_{Lbg})}(t) + w^{2apx}_{(1),(M_{Lbg})}(t) \tag{40}$$

Results for the beam displacement are presented in Fig. 18÷20.

- **All components of the beam displacement** $w^{2apx}_{(1),(G_{Lbg})st}(t), w^{2apx}_{(1),(G_{Lbg})dyn}(t)$ **and** $w^{2apx}_{(1),(M_{Lbg})st}(t), w^{2apx}_{(1),(M_{Lbg})dyn}(t)$.

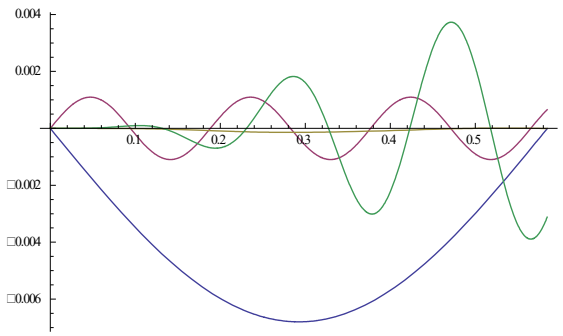

Fig. 18: Axes: x= t [s], y= All components [m], $w^{2apx}_{(1),(G_{Lbg})st}(L_b/2,t)$ - the blue colour, $w^{2apx}_{(1),(G_{Lbg})dyn}(L_b/2,t)$ - the brick red colour, $w^{2apx}_{(1),(M_{Lbg})st}(L_b/2,t)$ - the yellow colour, $w^{2apx}_{(1),(M_{Lbg})dyn}(L_b/2,t)$ - the green colour.

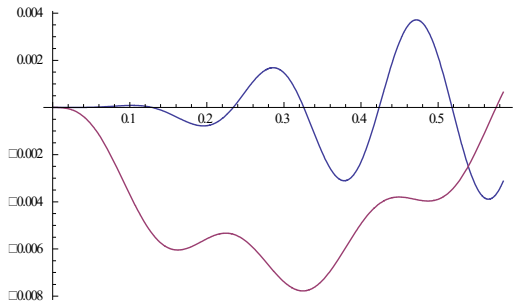

Fig. 19: Axes: x= t [s], y= Cumulative components [m], $w^{2apx}_{(1),(G_{Lbg})st}(L_b/2,t)$ - the blue colour, $w^{2apx}_{(1),(G_{Lbg})dyn}(L_b/2,t)$ - the brick red colour.

- **Cumulative components** $w^{2apx}_{(1),(G_{Lbg})}(L_b/2,t)$ **and** $w^{2apx}_{(1),(G_{Lbg})}(L_b/2,t)$ **for the mid-point of the beam**

The result of the cumulative components from Eq. (40) is presented in Fig. 19.

- **Total beam deflection at mid-span** $w^{2apx}_{(1),(G_{(Lbg)}+M_{Lbg})}(L_b/2,t)$ **due to load** $(G_{L_{bg}} + M_{L_{bg}})$, Fig. 20.

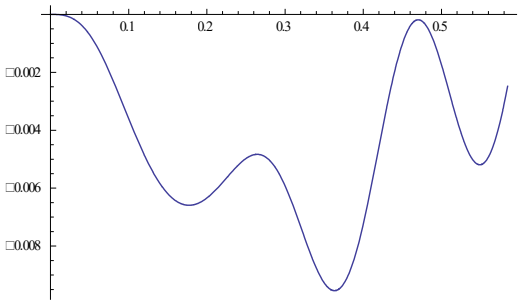

Fig. 20: Axes: x= t [s], y= Total beam displacement $w^{2apx}_{(1)(G_{Lbg}+M_{Lbg})}(L_b/2,t)$ [m], $\hat{w}^{2apx}_{(1)(G_{Lbg}+M_{Lbg})}(L_b/2,t) = 0.0098m$.

- **Dynamic coefficient** $\delta^{2apx}_{dyn}(L_b/2,t)$ **for the beam displacement, for the load** $(G_{L_{bg}} + M_{L_{bg}})$

The dynamic coefficient is defined as the ratio of the maximum dynamic deflection to the static deflection at mid-span of the beam. For the second iteration of the beam displacement it is

$$\delta^{2apx}_{dyn}(L_b/2,t) = \frac{w^{2apx}_{(1),(G_{Lbg}+M_{Lbg})\max}(L_b/2,t)}{w^{2apx}_{(1),(G_{Lbg,st})}(L_b/2,t)} \tag{41}$$

From the above dynamic analysis results the dynamic coefficient is show on Fig. 21.

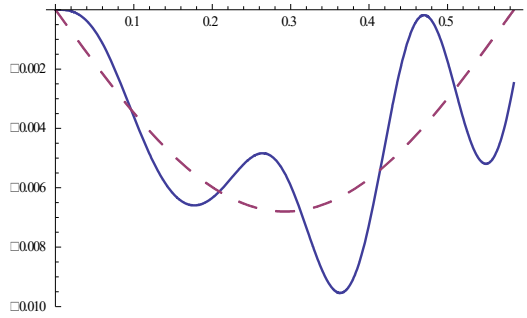

Fig. 21: Axes: x= t [s], y= Dynamic coefficient $\delta^{2apx}_{dyn}(L_b/2,t)$

$$\delta^{2apx}_{dyn}(L_b/2,t) = \frac{w^{2apx}_{(1),(G_{Lbg}+M_{Lbg})\max}(L_b/2,t)}{w^{2apx}_{(1),(G_{Lbg}st)}(L_b/2,t)} = \frac{0.0095}{0.0067} = 1.41$$

3.3 Comparison Results of Dynamic Response

- **Total interaction force $F^{2apx}_{(G_{Lbg}+M_{Lbg})}(p=ct)$ due to the mass moving load $(G_{L_{bg}}+M_{L_{bg}})$,** Fig. 22.

The total interaction force consist from the static contact force $G_{(L_{bg})}$ and the time-dependent dynamic component $F^{2apx}_{(M_{Lbg})}(p,t)$

$$F^{2apx}_{(G_{Lbg}+M_{Lbg})}(p,t)=G_{(L_{bg})}+F^{2apx}_{(M_{Lbg})}(p,t) \qquad (42)$$

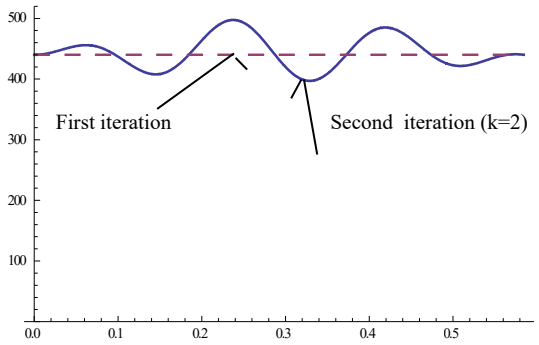

Fig. 22: Axes: x= t [s], y= Total interaction force $F^{2apx}_{(G_{Lbg}+M_{Lbg})}(p=ct)$ [kN], $\hat{F}^{2apx}_{(G_{Lbg}+M_{Lbg})}(p,t)=$ 496 kN.

- **Beam deflections at mid-span $q^{2apx}_{(1),(G_{Lbg})}(t)$ for (k=2) and $w^{2apx}_{(1),(G_{Lbg}+M_{Lbg})}(L_b/2,t)$ for (k=2),** Fig. 23.

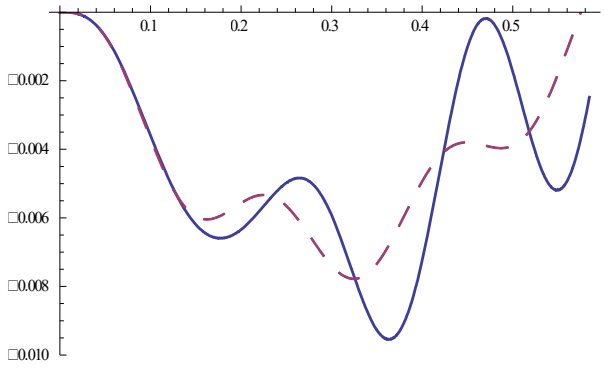

Fig. 23: Axes: x= t [s], y= Total beam displacements [m], $w^{2apx}_{(1),(G_{Lbg})}(L_b/2,t)$ - - - - - - $w^{2apx}_{(1),(G_{Lbg}+M_{Lbg})}(L_b/2,t)$ ———

Amplitudes: $\hat{w}^{2apx}_{(1)(G_{Lbg}+M_{Lbg})}(L_b/2,t)=0.0096$ m ,

$\hat{w}^{2apx}_{(1),(G_{Lbg})}(L_b/2,t)=0.0077m$

The ratio of amplitudes:

$$\Delta\left(\frac{w^{2apx}_{(1)(G_{Lbg}+M_{Lbg})}(L_b/2,t)}{w^{2apx}_{(1)(G_{Lbg})}(L_b/2,t)}\right)=\frac{0.0096}{0.0077}=1.24 \quad \text{..... 24 \%}$$

Dynamic coefficients:

$$\delta^{1apr}_{dyn}=\frac{0.0077}{0.0068}=1.13 \quad \text{and} \quad \delta^{2apx}_{dyn,(G_{Lbg}+M_{Lbg})}=\frac{0.0096}{0.0068}=1.41$$

3.4 Third Interaction (*k*=3)

This load state corresponds to the moving force $F^{3apx}_{(G_{Lbg}+M_{Lbg})}(p,t)$ and the beam deflections $w^{3apx}_{(G_{Lbg}+M_{Lbg})}(p,t)$ again can be solved superposition by analogy as in section 2. The main result for the mid-span of the beam is in Fig. 24.

- **Beam deflections at mid-span for (k=3)** $w^{3apx}_{(1),(G_{Lbg,st})}(L_b/2,t)$ and $w^{3apx}_{(1),(G_{Lbg}+M_{Lbg})}(L_b/2,t)$, Fig. 24

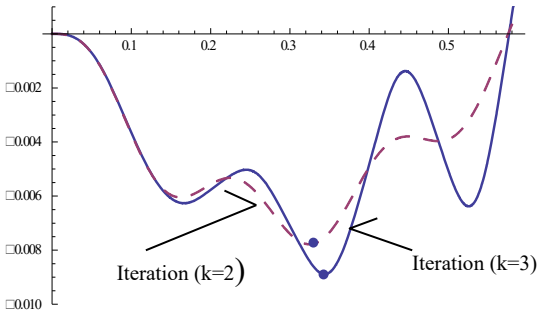

Fig. 24: Axes: x= t [s], y= Total beam displacements [m] , $w^{3apx}_{(1),(G_{Lbg})}(L_b/2,t)$ - - - - - - $w^{3apx}_{(1),(G_{Lbg}+M_{Lbg})}(L_b/2,t)$ ———,

Amplitudes: $w^{(3)apx}_{(1),(G_{Lbg}+M_{Lbg})}(L_b/2,t)=0.0089$ m

$\hat{w}^{3apx}_{(1)(G_{Lbg})}(L_b/2,t)=0.0077m$

$$\delta^{2apr}_{dyn}=\frac{0.0077}{0.0068}=1.13 \quad \text{and} \quad \delta^{(3)apx}_{(G_{Lbg}+M_{Lbg})dyn}(L_b/2,t)=\frac{0.0089}{0.0068}=1.31$$

- **Comparison Beam Deflections $w^{2apx}_{(1),(G_{Lbg}+M_{Lbg})}(L_b/2,t)$ for (k=2) and $w^{3apx}_{(1),(G_{Lbg}+M_{Lbg})}(L_b/2,t)$ for (k=3),** Fig. 25.

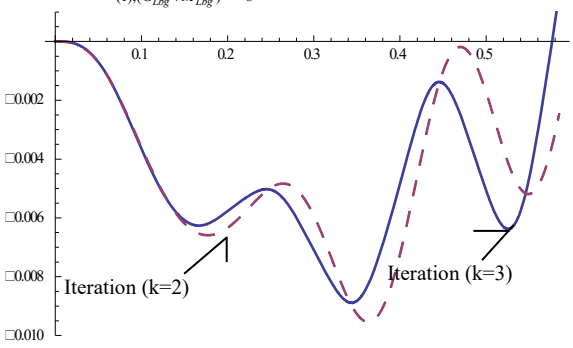

Fig. 25: Axes: x= t [s], y= Total beam displacements [m] , $w^{2apx}_{(1),(G_{Lbg}+M_{Lbg})}(L_b/2,t)$ for (k=2) – the blue colour

$w^{3apx}_{(1),(G_{Lbg}+M_{Lbg})}(L_b/2,t)$ for (k=3) – the red colour

Amplitudes: $\hat{w}^{2apx}_{(1)(G_{Lbg}+M_{Lbg})}(L_b/2,t)=0.0096$ m , :

$\hat{w}^{3apx}_{(1)(G_{Lbg}+M_{Lbg})}(L_b/2,t)=0.0089$ m .

4 Conclusion

The objective of this study was detailed analysis of the dynamic response of the real steel railway bridge, modelled as the simple supported beam and excited by the traversed mass load M_{Lbg} = 44 *t* concentrated at the locomotive bogies (Fig. 2,3), moving with the speed *c = 65 m/s = 234 km/h.* The influence of the individual components of the dynamic response, in particular, the effect of the quasi-static and dynamic components of the inertia force of the un-sprung mass on the dynamic response was study.

The following conclusions can be extracted:

(1) The iterative modal approach as an approximate solution is suitable tool for the practical analysis of a moving mass problem. One of the main features of the presented method is the capability of handling the nonlinear problems into the linear solution.

(2) The numerical solution demonstrated the efficiency of the iteration procedure allows to evaluate the influence of the moving mass on the dynamic response of the bridge. The numerical solution confirms that the third iteration gives adequate results.

(3) The time histories of the bridge displacement at the mid-span and dynamic coefficients determined from them showed that the mass vibration significantly affects the dynamic response, especially for the higher speeds. While the dynamic coefficient for the moving load is $\delta^{1apx}_{dyn(G_{Lbg})}(L_b/2,t)=1.13$, (Fig. 7), the dynamic coefficient due to the moving mass for (k = 2) is $\delta^{2apx}_{dyn(G_{Lbg}+M_{Lbg})}(L_b/2,t)=1.41$, (Fig. 21), and $\delta^{3apx}_{dyn(G_{Lbg}+M_{Lbg})}(L_b/2,t)=1.31$ for (k = 3)

(4) The influence of inertial effect of the mass at a higher speed influences the dynamic response especially when passing through the second half of the beam, when the inertial effects of the mass are significantly.

(5) The total response due to a moving vehicle obtains by utilization "the presented single concentrated bogies load" and the superposition principle with the application of the Heaviside function.

Acknowledgements

This study was supported by the Grant VEGA No. 1/0045/19 of the Grant Agency of the Slovak Republic.

References

[1] KOLOUŠEK V. *Monograph.* Dynamics of structures I. Publisher: SNTL Praha 1954, p. 263 (in Czech).

[2] BIGGS J.M. *Monograph*. Structural mechanics. Publisher: McGRAW-HILL, N.Y. ISBN 07005255-7, N.Y. 1964.

[3] Y.B.Yang, J.D.Yau, Y.S.Wu. Vehicle-Bridge Interaction Dynamics, https://doi.org./10.1142/5541/juli 2004.

[4] MORAVČÍK Milan, MORAVČÍK Martin. Resonance vibration of railway bridges subjected to passing vehicles. *Journal.* Scientific letters of the university of Žilina, Vol. 19, No.3 (2017), pp. 96÷101.

[5] MORAVČÍK Milan, Acceleration response of railway bridges –verification of the limit state of acceleration. *Journal.* Scientific letters of the university of Žilina, Vol. 21, No. 1/2019, pp. 59÷67.

[6] Wolfram Mathematics 10.0, Program system for technical computing.